Supplementary information for:

Visualization of codon-dependent conformational rearrangements during translation termination

Shan L. He[1] and Rachel Green[1]

[1]Howard Hughes Medical Institute, Department of Molecular Biology and Genetics, Johns Hopkins University School of Medicine, Baltimore, MD, 21205

Correspondence should be addressed Rachel Green: ragreen@jhmi.edu

Running title: Conformational rearrangements induced by RF1 codon recognition

Keyword: Ribosome, termination, release factor, conformational rearrangement, hydroxyl radical probing

Supplementary Figure 1

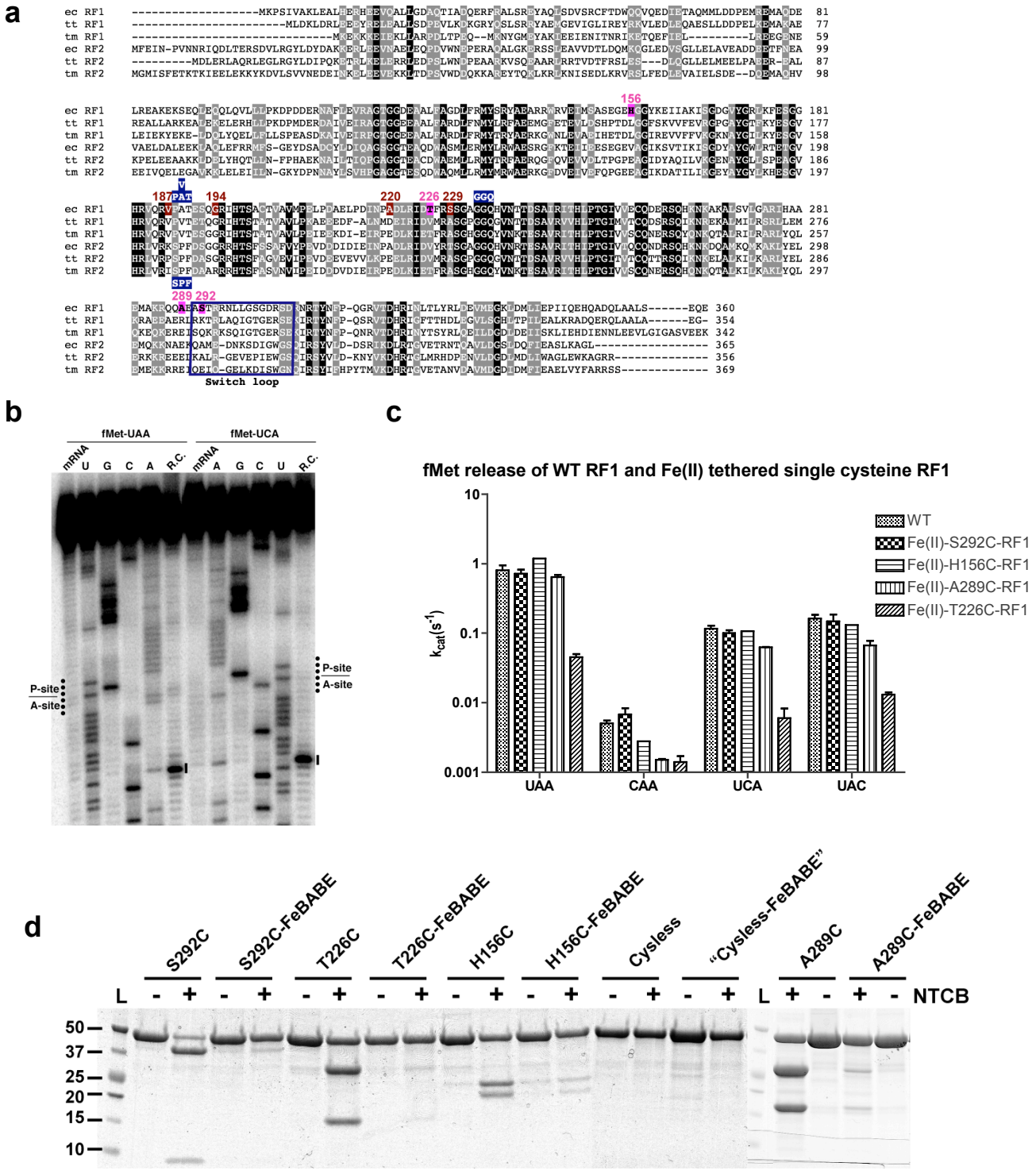

Supplementary Figure 1. Identification of candidate single cysteine RF1 variants for probing structural differences between authentic stop- and near-stop- codon complexes. (a) Alignment of several bacterial class 1 RF variants; *E. coli* (ec), *T. thermophilus* (tt), and *T. maritima* (tm). Extremely conserved residues are highlighted in black and somewhat less conserved residues in grey. Functionally important motifs including tripeptide anticodon (PV/AT or SPF), catalytic GGQ and swith loop are labeled in blue. The four single cysteine RF1 variants chosen for thorough characterization are labeled in pink while the ones that were discarded are shown in dark red. (b) Toeprinting analysis of the ribosome complexes (UAA or UCA at second codon). Lanes (U, G, C and A) indicate sequencing lane for the mRNA. (mRNA) represents a primer extension reaction on just the mRNA of interest. (R.C.) represents a primer extension reaction on the ribosome complex with mRNA positioned by $tRNA^{fMet}$ in the P site. The positions of the P-site and A-site codons are labeled on the sides of the gel and the position of the toeprint is highlighted by a black bar. (c) Functional characterization of Fe(II)-derivatized single-cysteine RF1 variants by *in vitro* peptide release assay. The bar graph shows the rate constants for catalysis at saturating release factor concentrations (k_{cat}) for wild-type RF1 and derivatized single cysteine RF1 mutants on (UAA) stop- or (CAA, UCA and UAC) near-stop-programmed ribosomes. Bars represent the mean ± standard error from at least two experiments. (d) SDS-PAGE gel of NTCB cleavage analysis of FeBABE derivatization efficiency. (L) is a protein ladder with molecular weights indicated on the left. (+) or (-) lanes represent samples where NTCB reagent was included, or not.

Supplementary Figure 2

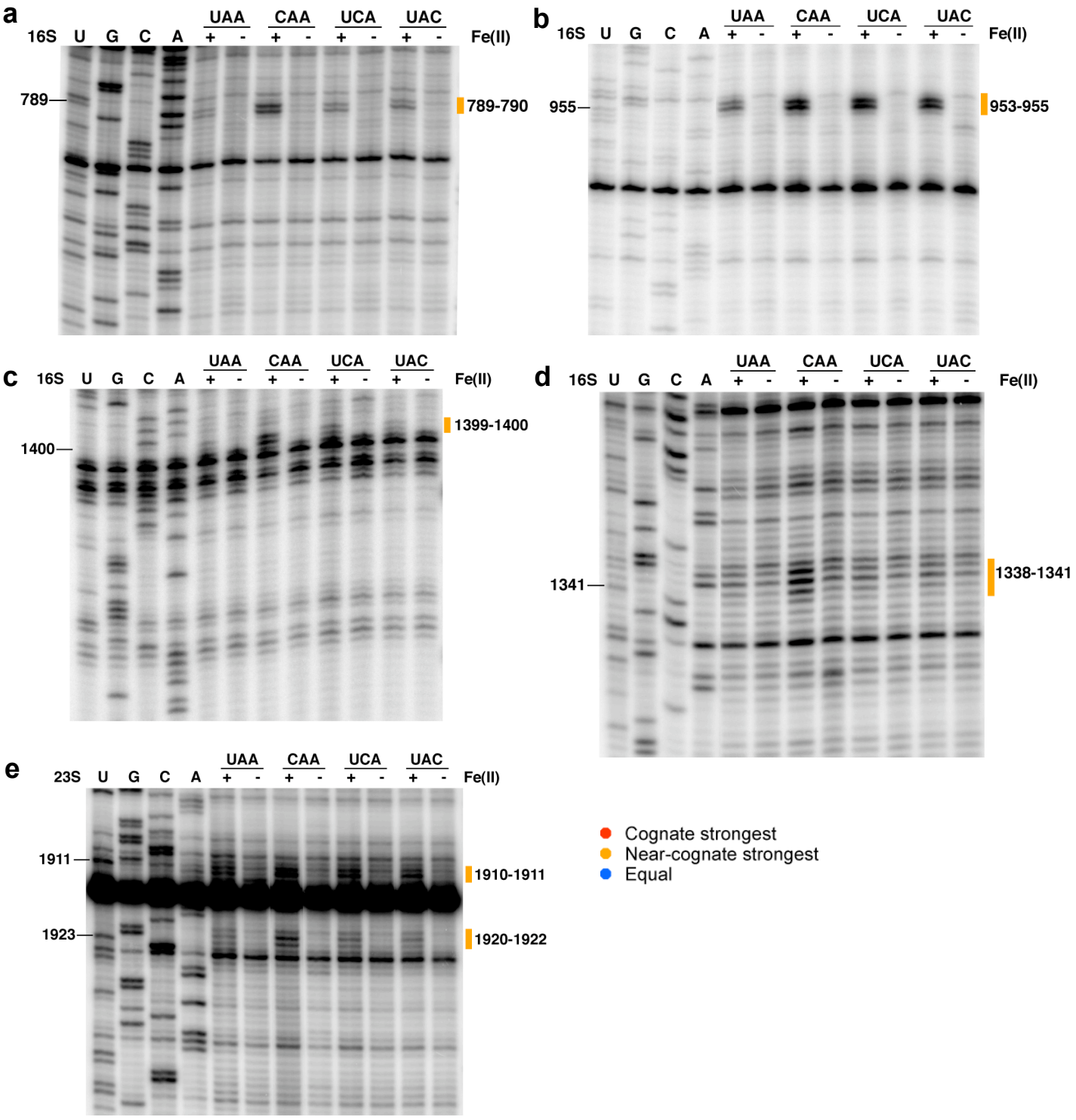

Supplementary Figure 2. Primer extension analysis of cleavage pattern of 16S rRNA (a-d) and 23S rRNA (e) from saturating levels of Fe(II)-H156C-RF1 in ribosome complexes with UAA, CAA, UCA or UAC codons in the A site. (U, G, C and A) are sequencing lanes. (+) represents the Fe(II)-H156C-RF1 sample while (–) represents the sample treated with mock labeled Cysless-RF1. Primers used begin at position 906 (a), 1046 (b), 1490 (c) and 1391 (d) of 16S rRNA and 2042 (e) of 23S rRNA. Bars and numbers at right indicate cleavages corresponding to nucleotides within 16S rRNA or 23S rRNA.

Supplementary Figure 3

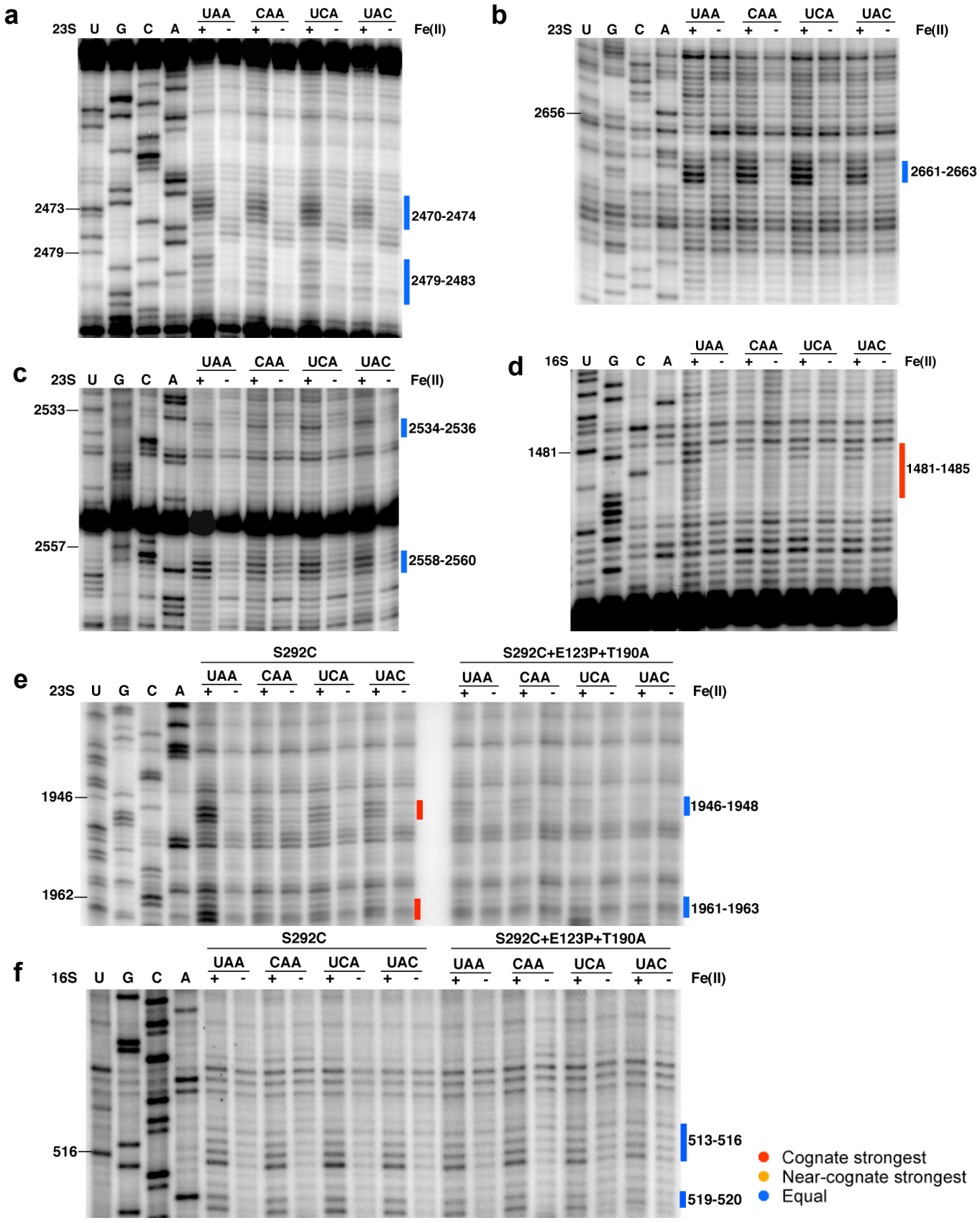

Supplementary Figure 3. Primer extension analysis of cleavage pattern of 23S rRNA (a-c and e) and 16S rRNA (d, f) from saturating levels of Fe(II)-S292C-RF1 with or without the indicated mutations in ribosome complexes with UAA, CAA, UCA or UAC codons in the A site. (U, G, C and A) are sequencing lanes. (+) represents the Fe(II)-S292C-RF1 (with or without the indicated mutations) sample while (–) represents the sample treated with mock labeled Cysless-RF1. Primers used begin at position 2542 (a), 2741 (b), 2639 (c) and 2042 (e) of 23S rRNA as well as 1508 (d) and 565 (f) of 16S rRNA. Bars and numbers at right indicate cleavages corresponding to nucleotides within 16S and 23S rRNA.

Supplementary Figure 4

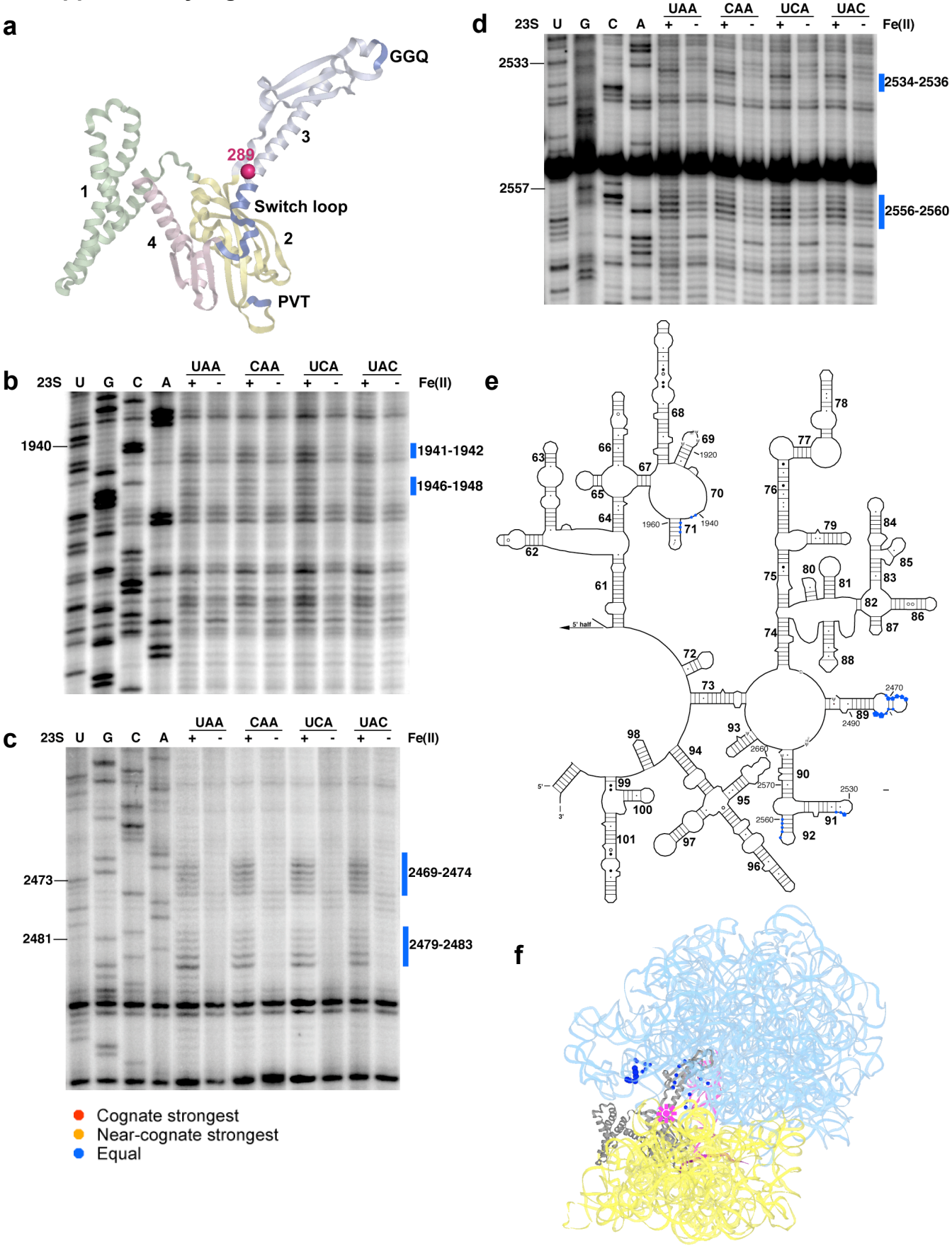

Supplementary Figure 4. Directed hydroxyl radical probing of the ribosome environment near position 289 (next to the switch loop of RF1) in ribosome complexes programmed with various codons in the A site. (a) Ribbon diagram of RF1. Sphere indicates Cα of residue 289 where Fe(II) is tethered. (b-d) Primer extension analysis of cleavage of 23S rRNA from saturating levels of Fe(II)-A289C-RF1 incubated with the indicated ribosome complexes with primers beginning at position (b) 2042, (c) 2542 and (d) 2639. (U, G, C and A) are sequencing lanes. (+) represents the Fe(II)-A289C-RF1 sample while (–) represents the sample treated with mock labeled Cysless-RF1. Bars and numbers at right indicate cleavages corresponding to nucleotides within 23S rRNA. (e) Directed hydroxyl radical cleavage sites from Fe(II)-A289C-RF1 displayed on the secondary structure of the 3' half of 23S rRNA. (g) All cleavage sites modeled on tertiary structure of RF1 bound ribosome complex (PDB entry: 3D5A and 3D5B), as in Figure 1.

Supplementary Figure 5

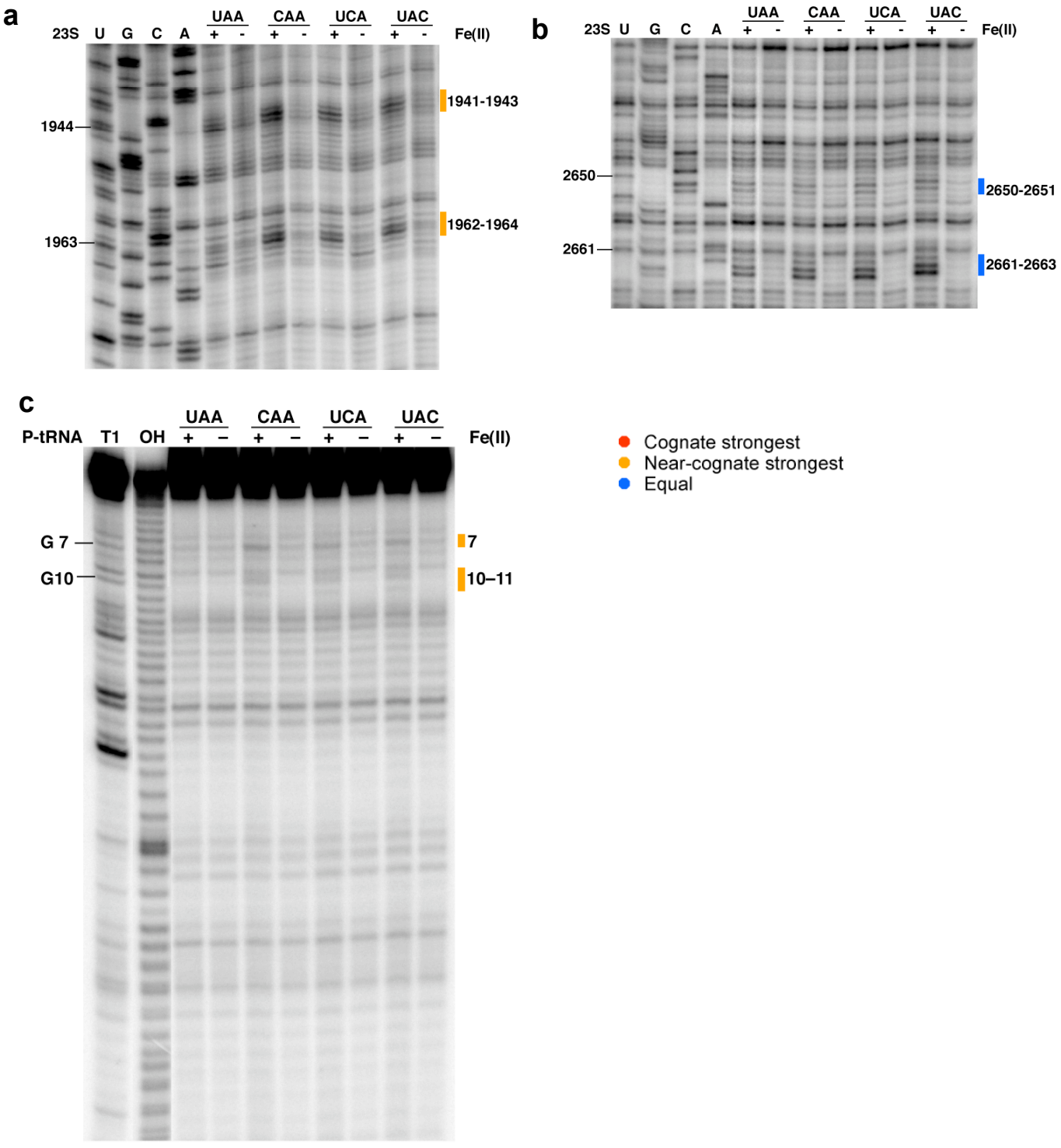

Supplementary Figure 5. Primer extension analysis and denaturing sequencing gel analysis of cleavage pattern of 23S rRNA (a-b) and P-site tRNA (c) from saturating levels of Fe(II)-T226C-RF1 in ribosome complexes with UAA, CAA, UCA or UAC codons in the A site. (U, G, C and A) are sequencing lanes. (+) represents the Fe(II)-T226C-RF1 sample while (–) represents the sample treated with mock labeled Cysless-RF1. Primers used are 2042 (a) and 2741 (b). (c) Denaturing sequencing gel analysis of cleavage of P-site tRNA from Fe(II)-T226C-RF1. (T1) cleavage by RNaseT1; (OH) alkaline hydrolysis ladder. Bars and numbers at right indicate cleavages corresponding to nucleotides within 23S rRNA or P-site tRNA.

Supplementary Figure 6

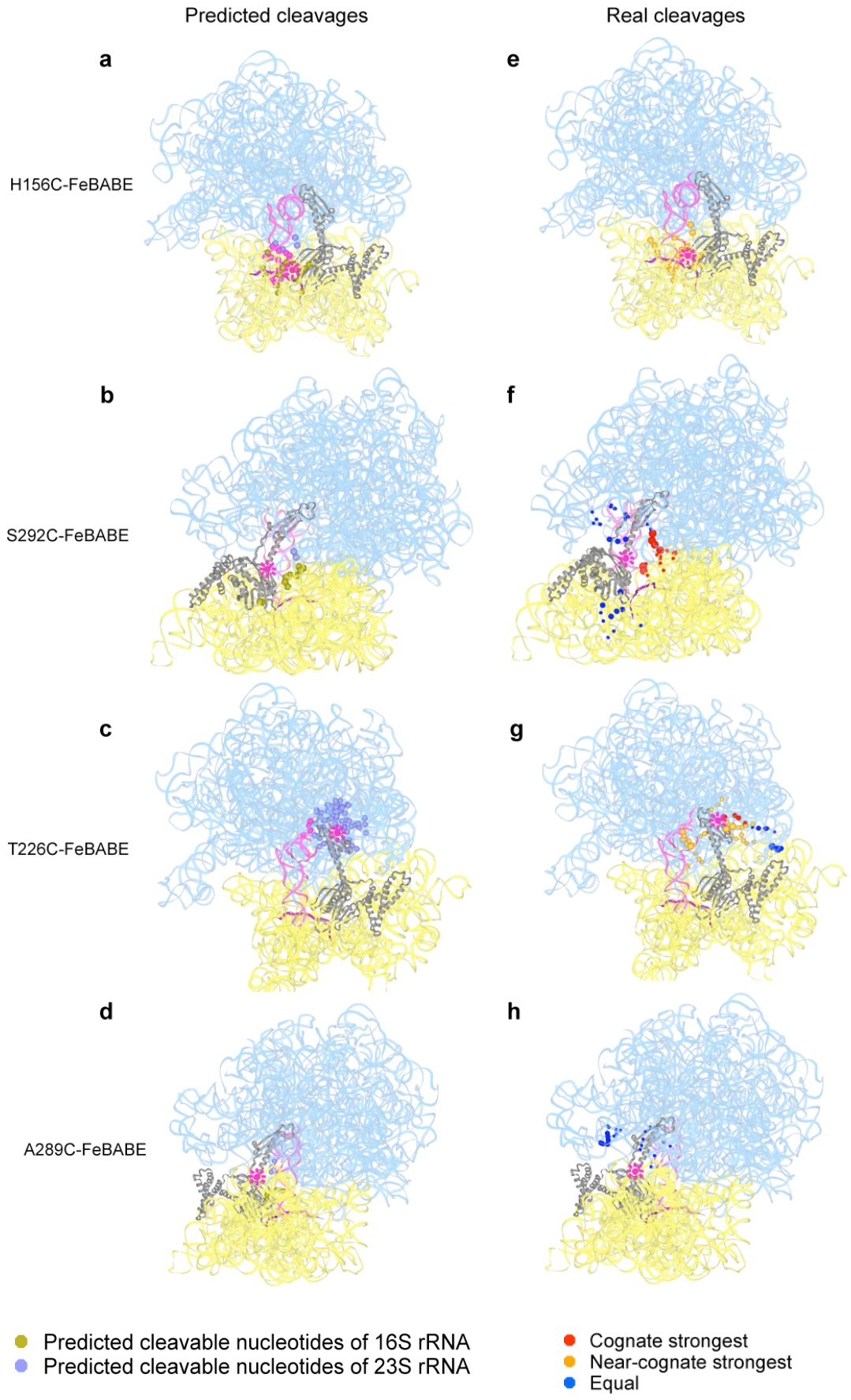

Supplementary Figure 6. Comparison of the predicted cleavable nucleotides (a-d) and the observed cleaved nucleotides (e-h) by hydroxyl radicals from position 156 (a, e), 292 (b, f), 226 (c, g) and 289 (d, h). Cleavable nucleotides were predicted by locating all the nucleotides within probing range (24 Å) of the positions where Fe(II) is tethered based on reported crystal structures (PDB entry: 3D5A and 3D5B). Predicted nucleotides of 16S rRNA are shown in olive green while those of 23S rRNA are shown in light blue. Observed cleavages are colored as throughout the paper; cleavages stronger on cognate (red), stronger on near-cognate (orange), and equivalent on all (blue).